



Nuclear stopping and rapidity loss in Au + Au collisions at $\sqrt{s_{NN}} = 62.4$ GeV

I.C. Arsene^k, I.G. Bearden^f, D. Beavis^a, S. Bekele^j, C. Besliuⁱ, B. Budick^e, H. Bøggild^f, C. Chasman^a, C.H. Christensen^f, P. Christiansen^{f,1}, H.H. Dalsgaard^{f,*}, R. Debbe^a, J.J. Gaardhøje^f, K. Hagel^g, H. Ito^a, A. Jipaⁱ, E.B. Johnson^{j,2}, C.E. Jørgensen^f, R. Karabowicz^d, N. Katrynska^d, E.J. Kim^{j,3}, T.M. Larsen^f, J.H. Lee^a, G. Løvholden^k, Z. Majka^d, M.J. Murray^j, J. Natowitz^g, B.S. Nielsen^f, C. Nygaard^f, D. Pal^j, A. Qviller^k, F. Rami^b, C. Ristea^f, O. Risteaⁱ, D. Röhrich^h, S.J. Sanders^j, P. Staszczak^d, T.S. Tvetter^k, F. Videbæk^{a,4}, R. Wada^g, H. Yang^h, Z. Yin^{h,5}, I.S. Zgura^c

^a Brookhaven National Laboratory, Upton, NY, USA

^b Institut Pluridisciplinaire Hubert Curien, IN2P3-CNRS et Université de Strasbourg, Strasbourg, France

^c Institute of Space Science, Bucharest-Magurele, Romania

^d M. Smoluchowski Inst. of Physics, Jagiellonian University, Krakow, Poland

^e New York University, NY, USA

^f Niels Bohr Institute, University of Copenhagen, Copenhagen, Denmark

^g Texas A&M University, College Station, TX, USA

^h University of Bergen, Department of Physics and Technology, Bergen, Norway

ⁱ University of Bucharest, Romania

^j University of Kansas, Lawrence, KS, USA

^k University of Oslo, Department of Physics, Oslo, Norway

ARTICLE INFO

Article history:

Received 30 December 2008

Received in revised form 8 April 2009

Accepted 23 May 2009

Available online 29 May 2009

Editor: V. Metag

PACS:

25.75.Dw

ABSTRACT

Transverse momentum spectra of protons and anti-protons measured in the rapidity range $0 < y < 3.1$ from 0–10% central Au + Au collisions at $\sqrt{s_{NN}} = 62.4$ GeV are presented. The rapidity densities, dN/dy , of protons, anti-protons and net-protons ($N_p - N_{\bar{p}}$) have been deduced from the spectra over a rapidity range wide enough to observe the expected maximum net-baryon density. From mid-rapidity to $y = 1$ the net-proton yield is roughly constant ($dN/dy \sim 10$), but rises to $dN/dy \sim 25$ at $2.3 < y < 3.1$. The mean rapidity loss is $2.01 \pm 0.14 \pm 0.12$ units from beam rapidity. The measured rapidity distributions are compared to model predictions. Systematics of net-baryon distributions and rapidity loss vs. collision energy are discussed.

© 2009 Elsevier B.V. Open access under CC BY license.

In collisions between gold nuclei at the top energy ($\sqrt{s_{NN}} = 200$ GeV) of the Relativistic Heavy Ion Collider, RHIC, there is strong evidence of a state of matter characterized by partonic (quark and gluon) degrees of freedom and with properties similar

to that of a nearly perfect liquid [1–5]. The partons are produced copiously during the initial stages of the collisions and subsequently hadronize into the roughly 7000 [6] particles produced in central collisions. The energy required for producing these particles comes from the kinetic energy lost by the baryons in the colliding nuclei. Since $E = m_T \cosh y$, where $m_T = \sqrt{m^2 + p_T^2}$ is the transverse mass (p_T is the transverse momentum), and y is the rapidity, this energy loss is manifest as a loss in mean rapidity of these baryons.

The net-baryon yield can be estimated from the net-proton yield, which is taken as the difference between the measured yields of protons and anti-protons. The rapidity distribution of the net-protons after the collision then not only determines the energy available for particle production, but also yields information on the stopping of the ions due to their mutual interaction.

* Corresponding author.

E-mail addresses: canute@nbi.dk (H.H. Dalsgaard), videbaek@bnl.gov (F. Videbæk).

¹ Present address: Div. of Experimental High-Energy Physics, Lund University, Lund, Sweden.

² Present address: Radiation Monitoring Devices, Cambridge, MA, USA.

³ Present address: Division of Science Education, Chonbuk National University, Jeonju, Republic of Korea.

⁴ Spokesperson.

⁵ Present address: Institute of Particle Physics, Huazhong Normal University, Wuhan, China.

By having a measurement at an energy between the lower energy AGS ($\sqrt{s_{NN}} = 5$ GeV) and SPS ($\sqrt{s_{NN}} = 17$ GeV) data and the highest energy RHIC results ($\sqrt{s_{NN}} = 200$ GeV) [7–9], the development of rapidity and energy loss can be studied in greater detail. In this Letter, we present the first measurements of the rapidity loss of Au ions after central collisions at $\sqrt{s_{NN}} = 62.4$ GeV. The experimental arrangement of the BRAHMS detector at RHIC makes it possible to measure the distribution of net-protons over a rapidity interval $y = 0$ to $y = 3.1$. This rapidity range is wide enough to include the maximum proton rapidity density, in contrast to the situation at the RHIC top energy, where the beam rapidity is higher ($y_b = 5.4$ compared to 4.2 at 62 GeV) and where the acceptance of existing experiments does not include this peak. The situation at the lower energy therefore makes it possible to better determine the rapidity density distribution. Together with similar information from experiments at lower energies, and at the RHIC top energy, we conclude that the mean rapidity loss of ultra-relativistic heavy ions exhibits a slowly varying behavior as a function of beam energy from SPS energies on upwards.

The BRAHMS detector consists of two magnetic spectrometers: the Mid Rapidity Spectrometer (MRS) able to cover polar angles (measured with respect to the beam direction) $30^\circ < \theta < 90^\circ$ and the Forward Spectrometer (FS) able to cover $2.3^\circ < \theta < 15^\circ$. Each spectrometer determines trajectories and momenta of charged hadrons. Two Time Projection Chambers (TPCs) are utilized in the MRS and two TPCs and three Drift Chambers (DCs) in the FS. Together, they measure protons and anti-protons in the range $-0.1 < y < 3.5$. Collision centrality is determined using a silicon and plastic tile multiplicity array located around the nominal intersection point (NIP) [6]. For this analysis, the centrality class 0–10% was selected, corresponding to a calculated number of participant nucleons of $N_{part} = 314 \pm 8$. The vertex position is determined with an accuracy of ≈ 1 cm using two arrays of Cherenkov counters positioned on either side of the NIP [10]. We have selected for analysis tracks in the MRS (FS) with vertices within $\pm 15(20)$ cm from the NIP.

Particle identification (PID) is done in the MRS via time of flight (TOF) measurements, enabling clean identification of protons and anti-protons in the momentum range $0.4 < p < 3$ GeV/c.

In the FS, two PID detectors are used: A TOF system and a Ring Imaging Cherenkov (RICH) detector. In the RICH, only (anti-)protons with $p > 15$ GeV/c can create resolvable rings. Lower momentum (anti-)protons have no associated Cherenkov radiation. In this Letter we have two sets of FS data corresponding to two settings of the spectrometer which again corresponds to rapidities $y \sim 2.3$ and $y \sim 3$. For $y \sim 2.3$ we use the TOF for PID with the RICH as a veto detector. In the momentum range $3 < p < 7.5$ GeV/c we apply a 2 sigma cut about the (anti-)proton peak in the calculated mass spectrum based on the TOF measurement and require that the particle not be identified in the RICH as a pion. For $y \sim 3$ the RICH is used exclusively for PID in the momentum range $10 < p < 30$ GeV/c. For $15 < p < 30$ GeV/c we make a 2 sigma cut around the peak in the mass spectrum calculated from the ring radii. If there is no resolvable ring we select particles that fail to make rings so that for $10 < p < 17$ GeV/c the (anti-)protons are those particles with either no associated ring or a ring with a small radius. There is an overlap in momentum to catch (anti-)protons that fail to create a ring despite momenta of $p > 15$ GeV/c.

The timing resolution of the MRS TOF is 90 ± 5 ps and the timing resolution in FS is 95 ± 6 ps. The momentum resolution in FS is $\Delta p/p = 0.016 \cdot p/p_{ref}$ where p_{ref} is the reference momentum for a given field setting. At the 1/2 field where the $y \sim 3$ data were taken $p_{ref} = 11$ GeV/c. Overall the $\Delta p/p$ is 1–2% for all settings in FS. For the MRS $\Delta p/p \sim 0.014p$ at large p [11].

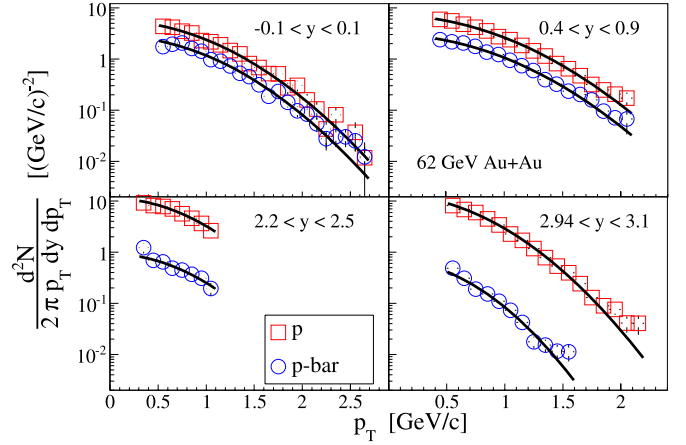


Fig. 1. Spectra of identified protons and anti-protons for $y \sim 0$, $y \sim 0.65$, $y \sim 2.3$ and $y \sim 3$ respectively. The solid drawn lines are the fit functions used to determine the yield. Vertical bars show statistical errors only.

The differential invariant yields, $\frac{1}{2\pi p_T} \frac{d^2N}{dy dp_T}$, of protons and anti-protons have been corrected for geometrical acceptance and detector efficiency. The acceptance correction is, due to the small solid angle of the BRAHMS spectrometers, the largest correction and is obtained from a purely geometrical simulation of each combination of angle and magnetic field used in the experiment. The PID efficiency of the TOF walls is found to be 93–98%. Since the RICH is 97% efficient for particles above threshold, up to 3% of pions and kaons in the momentum range $10 \text{ GeV/c} < p < 17 \text{ GeV/c}$ with ring radii zero will be mistakenly identified as protons, an effect for which we correct the data. This is done by first creating a spectrum of (anti-)kaons and (anti-)pions as if they were (anti-)protons. Then we subtract 3% of this spectrum from the (anti-)proton spectrum. The correction to protons is small, while for p -bar it amounts for up to 50% of the yield. Since the p -bar yield is small the effect on the net-protons is small. The total tracking efficiency in the MRS and FS is $\approx 90\%$ and $\approx 80\%$, respectively. The data have also been corrected for absorption, energy loss and multiple scattering estimated through simulations using GEANT [12]. The corrections for these physics effects amount to less than 20% at the lowest p_T and less than 15% at the highest p_T for the FS, whereas in the MRS the correction at the highest p_T is $\approx 8\%$.

Fig. 1 shows the invariant spectra of protons and anti-protons for $y \sim 0$, $y \sim 0.65$, $y \sim 2.3$ and $y \sim 3$ as a function of p_T . The integrated yields have been obtained by fitting these spectra with Gaussian functions ($f(p_T) \propto \exp(-p_T^2/2\sigma^2)$) and integrating the fit functions in the range $0 < p_T < \infty$. From the yields we obtain the rapidity densities $\frac{dN}{dy}$. The integrated yield under the data points compared to the extrapolated yield is ~ 80 –90% in the MRS and ~ 40 –50% in the FS. The mean p_T and m_T determined from the distributions varies from $\langle p_T \rangle \sim 1$ GeV/c ($\langle m_T \rangle \sim 1.4$ GeV) in the MRS to $\langle p_T \rangle \sim 0.7$ GeV/c ($\langle m_T \rangle \sim 1.2$ GeV) in the FS. The fits represent the data well. The spectra and the fits are consistent within 5% in the covered regions in p_T .

The top panel of Fig. 2 shows the dN/dy of protons and anti-protons. The lower panel shows the dN/dy of the net-protons, defined here as the difference of the proton and anti-proton densities. The systematic errors due to the limited p_T coverage have been found to be less than 7%. The main source of systematic uncertainties comes from the choice of fit function. We have used two alternative fit functions, a Boltzmann in m_T and an exponential in m_T , to estimate this systematic error. By varying the choice of fit functions we have found that this systematic error is

Download English Version:

<https://daneshyari.com/en/article/1853436>

Download Persian Version:

<https://daneshyari.com/article/1853436>

[Daneshyari.com](https://daneshyari.com)